Vol. 14, No. 4, 2023
ISSN 2233-4203/ e-ISSN 2093-8950
ARTICLE www.msletters.org | Mass Spectrometry Letters

# Investigation of the Copper (Cu) Binding Site on the Amyloid beta 1-16 (Aβ16) Monomer and Dimer Using Collision-induced Dissociation with Electrospray Ionization Tandem Mass Spectrometry

**Ji Won Jang, Jin Yeong Lim, Seo Yeon Kim, Jin Se Kim, and Ho-Tae Kim***

*Department of Chemistry and Bioscience, Kumoh National Institute of Technology, 61, Daehak-ro, Gumi, Gyeongbuk, Republic of Korea, 39177*

*Received November 13, 2023, Revised December 6, 2023, Accepted December 10, 2023*
*First published on the web December 31, 2023; DOI: 10.5478/MSL.2023.14.4.153*

**Abstract :** The copper ion, Cu(II), binding sites for amyloid fragment Aβ1-16 (=Aβ16 ) were investigated to explain the biological activity difference in the Aβ16 aggregation process. The $[M+Cu+(z-2)H]^{z+}$ (z = 2, 3 and 4, M = Aβ16 monomer) and $[D+Cu+(z-2)H]^{z+}$ (z = 3 and 5, D = Aβ16 dimer) structures were investigated using electrospray ionization (ESI) mass spectrometry (MS) and tandem mass spectrometry (MS/MS). Fragment ions of the $[M+Cu+(z-2)H]^{z+}$ and $[D+Cu+(z-2)H]^{z+}$ complexes were observed using collision-induced dissociation MS/MS. Three different fragmentation patterns (fragment "a", "b", and "y" ion series) were observed in the MS/MS spectrum of the (Aβ16 monomer or dimer—Cu) complex, with the "b" and "y" ion series regularly observed. The "a" ion series was not observed in the MS/MS spectrum of the $[M+Cu+2H]^{4+}$ complex. In the non-covalent bond dissociation process, the $[D+Cu+3H]^{5+}$ complex separated into three components ($[M+Cu+H]^{3+}$, $M^{3+}$, and $M^{2+}$), and the $[M+Cu]^{2+}$ subunit was not observed. The {M + fragment ion of $[M+Cu+H]^{3+}$} fragmentation pattern was observed during the covalent bond dissociation of the $[D+Cu+3H]^{5+}$ complex. The {M + $[M+Cu+H]^{3+}$} complex geometry was assumed to be stable in the $[D+Cu+3H]^{5+}$ complex. The {M + fragment ion of $[M+Cu]^{2+}$} fragmentation pattern was also observed in the MS/MS spectrum of the $[D+Cu+H]^{3+}$ complex. The {M + $[y_9+Cu]^{1+}$} fragment ion was the characteristic fragment ion. The $[D+Cu+H]^{3+}$ and $[D+Cu+3H]^{5+}$ complexes were likely to form a monomer-monomer-Cu (M-M-Cu) structure instead of a monomer-Cu-monomer (M-Cu-M) structure.

**Key words :** Aβ16, [Aβ16 monomer—Cu] complex, [Aβ16 dimer—Cu] complex, collision-induced dissociation (CID), mass spectrometry (MS), MS/MS

## Introduction

The Aβ protein, which shows an abnormal accumulation in patients with Alzheimer's disease (AD),[1–2] is one example of a misfolded protein. Because amyloid plaques occur particularly in AD patients, whereas the Aβ protein is usually present in healthy brains in a soluble form,[3] the aggregation process wherein the soluble Aβ protein forms plaques are the key step of the amyloid plaque formation process. It is currently conjectured that soluble, oligomeric forms of Aβ are more toxic species than aggregated fibrils or protofibrils.[4,5] However, the structure and formation process of Aβ oligomers are not yet understood clearly because of the metastable character of Aβ oligomers.[6] Aβ oligomer formation processes have been studied using various experimental and theoretical methods.[7–10]

Aβ plaques have been found to contain large amounts of transition metal cations such as Fe, Cu, and Zn ions.[11] Many studies have indicated that these transition metal ions are directly involved in the neurodegenerative disease.[12] Research has been conducted to show dys-homeostasis in the brain levels of Fe, Cu, and Zn ions and abnormalities in their metabolism in AD patients.[13] *In vitro* studies have revealed that these transition metals generally promote the aggregation of the Aβ protein.[14] Some studies have investigated the oxidative damage to proteins and peptides induced by Fe, Cu, and Zn metal ions.[15,16] Therefore, it is essential to determine the coordination sites of these metal ions at different charge states of the Aβ protein to understand their reactivity and show their potential role in the degeneration process.

Cu was found with high concentrations in amyloid



*Reprint requests to Ho-Tae Kim
https://orcid.org/0000-0002-1541-3081
E-mail: hotaekim@kumoh.ac.kr

plaques (~400 μM) compared to the normal brain extracellular concentration of ~1 μM.[11,13] Cu-induced Aβ aggregation is still controversial in relation to its accelerating and inhibiting effects in the aggregation process. It seems to depend on the experimental conditions and aggregational complex states.[17–18] Four possible (Aβ–Cu) complex geometries were proposed based on differences in the Cu coordination sites during the (Aβ–Cu ion) complexation process: Cu coordination sites of complex 1 geometry; Asp1-COO, N-terminus, His6, His13(or His14), complex 2 geometry; Asp1-COO, His6, His13, His14, complex 3 geometry; His6, Tyr10, His13, His14, complex 4 geometry; His13, His14.[19] It has been proposed that the metal ion binding site lies in the N-terminus domain, or more precisely in the first 16 amino acids of the Aβ protein. The Aβ16 peptide shows no tendency to aggregate or form fibrils under moderate concentrations. Therefore, an (Aβ16—metal ion) complex was also studied to understand the reactivity and functional group activity of the first 16 amino acids of the Aβ protein.[19]

In this study, we used collision-induced dissociation (CID) in conjunction with electrospray ionization (ESI)-mass spectrometry (MS) to obtain structural information about the (Aβ16 monomer or dimer—Cu) complex. The (Aβ16 monomer or dimer—Cu) complex was allowed to form in solution and were electrosprayed onto a quadrupole ion guide. A low-energy CID-MS/MS method was used to investigate the fragment ion species and patterns of multiply charged (Aβ16 monomer or dimer—Cu) complexes.

## Experimental

A Thermo Finnigan LTQ mass spectrometer (Thermo Fisher Scientific, Waltham, MA, USA) was used to obtain the MS and MS/MS spectra for the (Aβ16 monomer or dimer—Cu) fragmentation pattern analysis. The LTQ is a linear ion trap mass spectrometer equipped with an atmospheric pressure ESI source.

### MS Conditions

The (Aβ16 monomer or dimer—Cu) complex samples were introduced into the elctrospray interface by a direct infusion method using a microsyringe pump at a flow rate of 1 mL $min^{-1}$. The heated capillary temperature was set at 150°C to facilitate efficient complex formation. Positive-ion MS spectra were acquired over an *m/z* range of 100–2000 by averaging 1000–6000 scans. The MS/MS experimental conditions were as follows: ion-trap pressure, $1 \times 10^{-5}$ Torr; activation time, 30 ms; injection time, 100–200 ms; and isolation width, 0.7–1.5 mass units. The parent (Aβ16 monomer or dimer—Cu) complex ions were individually and manually selected and subjected to CID. The CID collision energies were optimized for each MS/MS experiment to obtain sufficient signal-to-noise ratios.

### Reagents

Aβ16 synthetic peptide (purity > 95%, amidated at the C-terminus DAEFRHDSGYEVHHQK-$NH_2$, Peptron, Daejeon, Korea), cupric chloride dihydrate (99%, Sigma-Aldrich Korea), and $H_2O$ (HPLC grade, Merck Ltd., Korea) were used in the experiments. The Aβ16 peptide and Cu solutions were prepared in water at a final concentration of 150 μM. These two solutions were mixed prior to obtaining the mass spectra. The solutions were prepared to achieve a sufficient $[D+Cu+H]^{3+}$ ion intensity for the CID-MS/MS experiments. The experiments were performed within 24 h of sample preparation.

## Results and Discussion

### MS Spectra

The ESI mass spectra of the (Aβ16–Cu) solutions indicated the presence of multiply charged (Aβ16 monomer or dimer—Cu) complexes, as shown in Figure 1. $[M+Cu]^{2+}$,

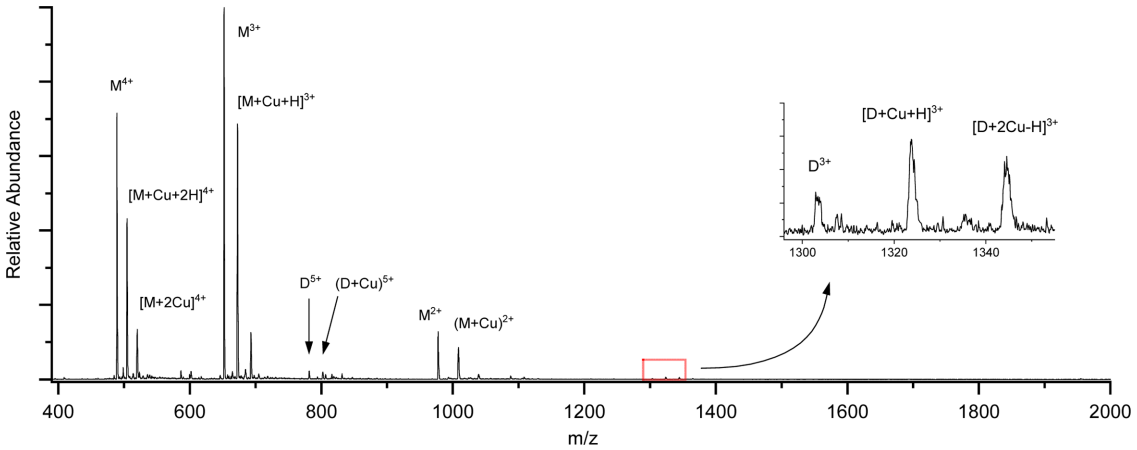


**Figure 1.** ESI-MS spectrum of (Aβ16—Cu) solution. Multiply charged monomers and dimers are represented as $[M+Cu+(z-2)H]^{z+}$ and $[D+Cu+(z-2)H]^{z+}$ (z = 2, 3, and 4 charge states, M = Aβ16 monomer, and D = dimer).

 

$[M+Cu+H]^{3+}$, and $[M+Cu+2H]^{4+}$ were observed at *m/z* 1007.9, 672.3, and 504.5, respectively, ranging from 2+ to 4+ in multiple proton adduct forms. The Aβ16 peptide contained five basic residues (Arg5, His6, His13, His14, and Lys16) and an N-terminus position, which were available for Cu coordination and protonation.

The observed $[M+Cu+H]^{3+}$ and $[M+Cu+2H]^{4+}$ peaks had high intensities, as seen in Figure 1. The observed $[M+2Cu-H]^{3+}$ and $[M+2Cu]^{4+}$ peaks, *m/z* 692.6 and 519.7, also had relatively high intensities in the 150 μM Cu concentration. For the Aβ16 dimers, peaks were observed at *m/z* 1323.2 and 794.3, corresponding to $[D+Cu+H]^{3+}$ and $[D+Cu+3H]^{5+}$, respectively. No [trimer or oligomer+Cu] peak was observed in the ESI-MS spectrum of our 150 μM (Aβ16—Cu) solution. It is supposed that the formation process for soluble forms of Aβ16 trimer (or oligomer)[20] was inhibited by the existence of the 150 μM Cu ion.

**MS/MS Spectra of (Aβ16 monomer—Cu)**

CID-MS/MS experiments were conducted to obtain structural information on the parent $[M+Cu+(z-2)H]^{z+}$ (z = 2, 3, and 4) ions. The fragment ions in the MS/MS spectra are labeled with various colors and shapes based on their charge states and fragment ion species in Figure 2. The *m/z* values and assignments of the fragment ions are presented in the Electronic Supplementary Information (Table S1). Three different fragmentation patterns (fragments "a", "b", and "y" ion series) were observed in the MS/MS spectrum of the (Aβ16 monomer—Cu) complex. The fragment "b" and "y" ion series were regularly observed in the MS/MS spectrum of the $[M+Cu+(z-2)H]^{z+}$ (z=2, 3 and 4) complex. However, the fragment "a" ion series was not observed in the MS/MS spectrum of $[M+Cu+2H]^{4+}$. These MS/MS fragmentation patterns of (Aβ16 monomer—Cu) will be useful for analyzing the (Aβ16 dimer—Cu) MS/MS spec-

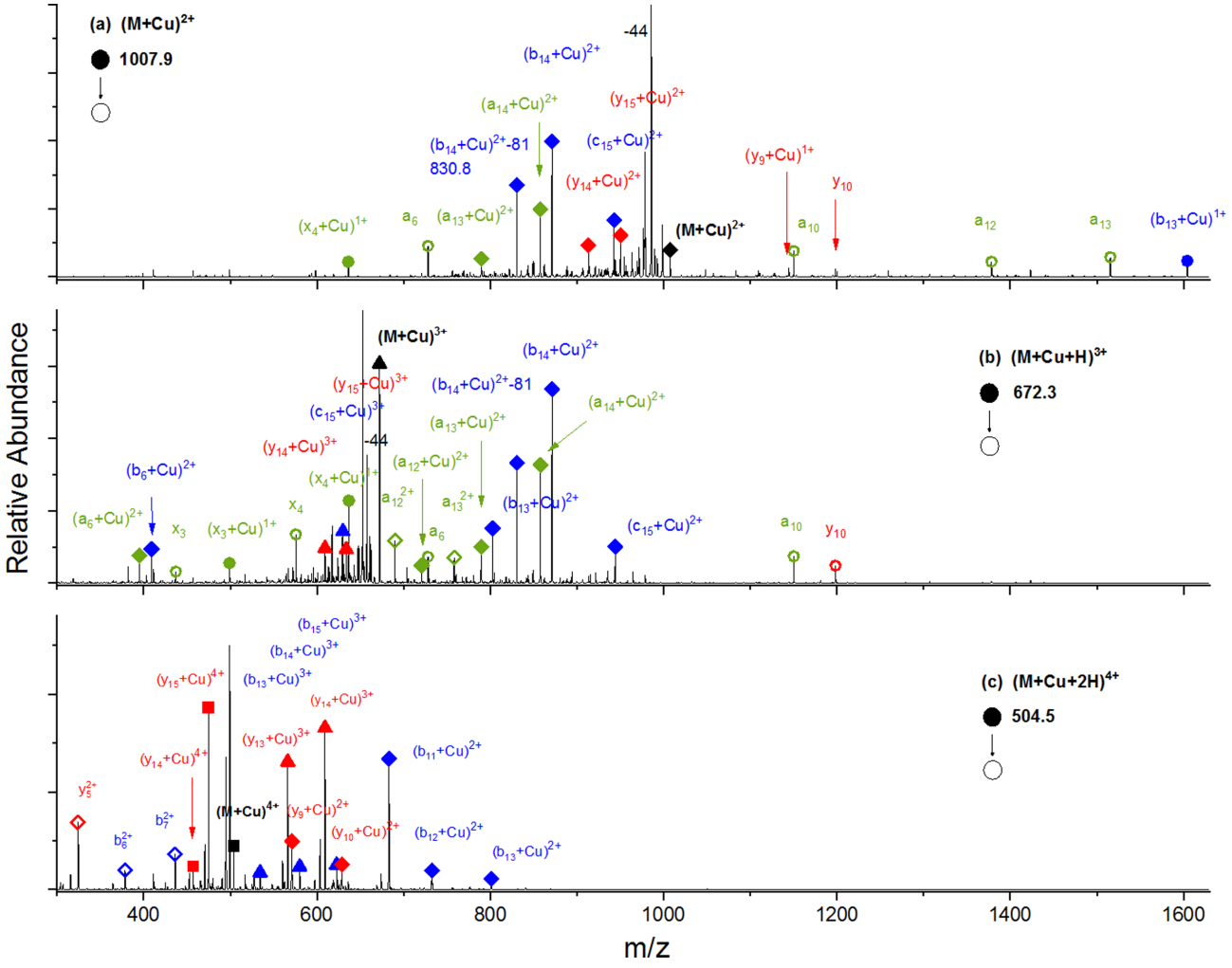


**Figure 2.** MS/MS spectra of (a) $[M+Cu]^{2+}$, (b) $[M+Cu+H]^{3+}$, and $[M+Cu+H]^{3+}$ parent ion. The charge states are distinguished by different shapes (1+ = circle, 2+ = diamond, 3+ = triangle, 4+ = square). The a, b, and y fragment ions are indicated by green, blue, and red colors, respectively. The filled shapes indicate the existence of Cu ions in fragment ions. For simplicity, (1+) charge state is omitted in the fragment "a" and "y" ion series, $a_{10}=a_{10}^{1+}$ and $y_{10}=y_{10}^{1+}$.

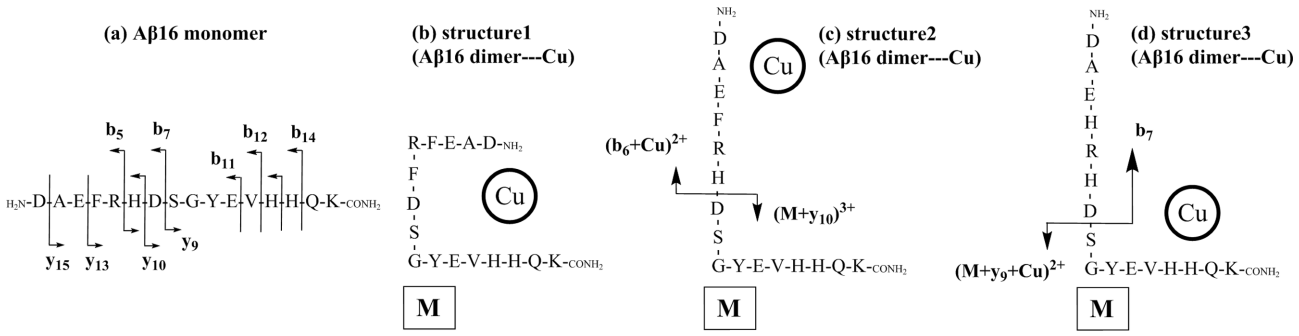


**Scheme 1.** Aβ16 monomer sequence along with fragmentation sites[20] and schematics of proposed (Aβ16 dimer—Cu) complex. Structures (b) 1 and (c) 2 correspond to the {M + ①, ②, or ③} and {M + ⑤} fragment ions in the MS/MS spectrum of $[D+Cu+3H]^{5+}$, respectively. (d) Structure 3 corresponding to the {M+ ④ $[y_9+Cu]^{1+}$} fragment ion in the MS/MS spectrum of $[D+Cu+H]^{3+}$.

trum. The Aβ16 sequence along with fragmentation sites[20] and three schematic (Aβ16 dimer—Cu) structures are proposed for the {M-M-Cu} geometry instead of {M-Cu-M} geometry in Scheme 1.

Fragment ions of the "a", "b", and "y" ion series are shown in Figure 2a as the MS/MS spectrum of the $[M+Cu]^{2+}$ complex. Similar MS/MS fragmentation patterns for $[M+Cu]^{2+}$ have been reported under different experimental conditions.[19] Two separate MS/MS fragmentation patterns have been reported according to the two possible geometric forms for the $[M+Cu]^{2+}$ complex, the complex 3 geometry (four coordination sites of Cu) and complex 4 geometry (two coordination sites of Cu). However, as shown in Figure 2a, the two separate MS/MS fragmentation patterns of the complex 3 and complex 4 geometries were observed simultaneously under our experimental conditions.

The simultaneous observation of these two MS/MS fragmentation patterns was attributed to the coexistence of the complex 3 and complex 4 geometries for $[M+Cu]^{2+}$. Under our air-exposed experimental conditions, atmospheric ESI spray source conditions and air-exposed sample preparation, it was assumed that the oxidation state of Cu was (+2) instead of (+1) in the $[M+Cu]^{2+}$ complex. The observed fragment ① $[M+Cu-44]^{2+}$ ion peak (Table 1) had a prominent intensity, as seen in Figure 2a. The 44 amu loss dissociation in the $[M+Cu]^{2+}$ complex was thought to occur as a $CO_2$ dissociation process from the side group of the Asp1 residue in $[M+Cu]^{2+}$. This analysis was based on the fragmentation patterns for [(fragment "a" and "b" ion series)-44] and [fragment "y" ion series ($y_{15}$ included)+Cu] in the MS/MS/MS spectrum of the $[M+Cu-44]^{2+}$ parent ions (Figure S1a).

The spectrum shown in Figure S1a indicates that the $[M+Cu-44]^{2+}$ fragment ions did not originate from the complex 1 or complex 2 geometry, which includes Asp1-COO as Cu coordination sites. The $CO_2$ loss dissociation process hardly occurred for the complex 1 or complex 2 geometry under our low-energy CID conditions because additional energy was needed to break the extra bond of Cu coordination at the Asp1- COO side group.

One peculiar observation in the MS/MS spectrum of the $[M+Cu]^{2+}$ complex was at *m/z* 830.8 in Figure 2a, which was also observed in the MS/MS spectrum of $[b_{14}+Cu]^{2+}$ (Figure S1b) and assigned to the $[b_{14}+Cu-81]^{2+}$ fragment ion (Table 1). The 81 amu loss was reported as a side group dissociation process of the histidine amino acid in the CID experimental results.[21] Therefore, an 81 amu loss could occur among the three histidine residues (His6, His13, and His14). In the $[b_{14}+Cu-81]^{2+}$ fragment ion, the 81 amu loss was thought to occur from the side group of the His14 residue, instead of at His6 or His13, because of the observation of *m/z* 790.2, which was assigned to the $[a_{13}+Cu]^{2+}$ fragment ion in the MS/MS/MS spectrum of the $[b_{14}+Cu-81]^{2+}$ ion (Figure S1c). If there is some competition between His13 and His14 in the complex 1 geometry, it is conjectured that the side group of His14 does not participate in the Cu coordination process in the complex 1 geometry based on the observation of the $[b_{14}+Cu-81]^{2+}$ fragment ion.

It is interesting to note that the "a" fragment ion series (③ $a_6$, $a_{10}$, $a_{12}$, and $a_{13}$ fragment ions, Table 1) can be observed in Figs. 2a–2b, while the fragment "a" ion series was not observed in the Aβ16 MS/MS spectrum.[20] These "a" fragment ions are supposed to originate from oxidative routes induced by the Cu positive ion. The potential formation of peptide radical through Cu coordination and "a" fragment ions in tandem mass spectra were reported by Ke et al.[21] An oxidation process based on the oxidation of nitrogen atoms at the peptide backbone has been reported by two research groups.[22–23] These unusual "a" fragment ions, the $C_\alpha$-C backbone cleavage, are usually observed in the photodissociation of singly charged cations[24] or in the electron-detachment dissociation of polyanions.[25]

The ④ $[y_9+Cu]^{1+}$ fragment ion (Table 1), *m/z* 1144.4 in Figure 2a, is one of the characteristic dissociation channels of the $[M+Cu]^{2+}$ complex. A weak bonding characteristic for the D7-S8 peptide bond was observed in the $[M+Cu]^{2+}$ MS/MS spectrum of the complex 4 geometry in the results

 

**Table 1.** Comparison of MS/MS fragment ions of (Aβ16 monomer—Cu) and (Aβ16 dimer—Cu). Fragment "a," "b," and "y" ions were observed in the MS/MS spectrum of (Aβ16 monomer—Cu). (M + a), (M + b), and (M + y) fragment ions were observed in the MS/MS spectrum of (Aβ16 dimer—Cu).

| Parent ion | MS/MS fragmentation patterns | | | |
|---|---|---|---|---|
| | "a" ion | "b" ion | "y" ion | Characteristic ions |
| $[M+Cu]^{2+}$ | $a_6$,$a_{10}$,$a_{12}$,$a_{13}$<br>$(a_{14}+Cu)^{2+}$ | $(b_{14}+Cu)^{2+}$ | $(y_{14}+Cu)^{2+}$<br>$(y_{15}+Cu)^{2+}$ | ① $(M+Cu-44)^{2+}$<br>② $(b_{14}+Cu-81)^{2+}$<br>③ $a_6$,$a_{10}$,$a_{12}$,$a_{13}$<br>④ $[y_9+Cu]$ |
| $[M+Cu+H]^{3+}$ | $a_6$,$a_{10}$, $a_{12}^{2+}$,$a_{13}^{2+}$<br>$(a_{12}+Cu)^{2+}$ $(a_{13}+Cu)^{2+}$<br>$(a_{14}+Cu)^{2+}$ | $(b_{13}+Cu)^{2+}$<br>$(b_{14}+Cu)^{2+}$ | $y_{10}$<br>$(y_{14}+Cu)^{3+}$<br>$(y_{15}+Cu)^{3+}$ | ① $(M+Cu-44)^{2+}$<br>② $(b_{14}+Cu-81)^{2+}$<br>③ $a_6$,$a_{10}$,$a_{12}$,$a_{13}$<br>⑤ $y_{10}$<br>⑥ $(a_6+Cu)^{2+}$, $(b_6+Cu)^{2+}$ |
| $[M+Cu+2H]^{4+}$ | N/A | observed | observed | ⑦ $y_5$ and ⑧ $[b_{11}+Cu]^{2+}$ |
| $[D+Cu+H]^{3+}$ | N/A | $b_7$ | $(M+y_{14}+Cu)^{3+}$ | M+ ③ , M+ ④ |
| $[D+Cu+3H]^{5+}$ | $[M+a_{12}]^{4+}$, $[M+a_{13}]^{4+}$<br>$[M+a_{12}+Cu]^{4+}$ $[M+a_{13}+Cu]^{4+}$<br>$(M+a_{14}+Cu)^{4+}$ | $(M+b_{13}+Cu)^{4+}$<br>$(M+b_{14}+Cu)^{4+}$<br>$(M+b_{14}+Cu)^{5+}$ | $(M+y_{10})^{3+}$<br>$(M+y_{13}+Cu)^{4+}$<br>$(M+y_{14}+Cu)^{4+}$<br>$(M+y_{14}+Cu)^{5+}$<br>$(M+y_{15}+Cu)^{5+}$ | M+ ①,<br>M+ ②,<br>M+ ③,<br>M+ ⑤,<br>⑥ |

reported by Lu et al.[19] The bond weakness of the D7-S8 peptide bond has also been observed in the Aβ16 MS/MS spectrum.[20] Therefore, it is conjectured that the weak bonding characteristic of the D7-S8 peptide bond is maintained in the $[M+Cu]^{2+}$ complex 4 geometry because of the small geometric difference between the complex 4 geometry and original Aβ16 geometry at the D7-S8 peptide bond area.

Figure 2b shows the MS/MS spectrum of the $[M+Cu+H]^{3+}$ complex. Three different fragmentation patterns (fragment "a", "b", and "y" ion series, Table 1) were found in the MS/MS spectrum of the $[M+Cu+H]^{3+}$ complex, similar to that for $[M+Cu]^{2+}$, while the charge states of the fragment "a", "b", and "y" ions were changed according to the basic residues for the one extra proton ($H^+$) addition process. The 44 and 81 loss fragments, ① $[M+Cu-44]^{3+}$ and ② $[b_{14}+Cu-81]^{2+}$ ions, were also observed in the spectrum shown in Figure 2b. The notable difference between Figs. 2a and 2b is that the ④ $[y_9+Cu]^{1+}$ fragment ion is absent in Figure 2b and new fragments of ⑤ $y_{10}$ and ⑥ $[a_6+Cu]^{2+}$ or $[b_6+Cu]^{2+}$ appear instead. These two new fragments cannot be explained by the complex 1–complex 4 geometries. Therefore, a hypothetical complex 5 geometry of $[M+Cu+H]^{3+}$, in which Cu is located at the D1-H6 sequences of the N-terminal vicinity area, is required to explain the fragment $[a_6+Cu]^{2+}$ or $[b_6+Cu]^{2+}$. The 3+ charge state of the (Aβ16—Cu) complex is assumed to be crucial to the dissociation process of the ⑤ $y_{10}$ and ⑥ $[a_6+Cu]^{2+}$ or $[b_6+Cu]^{2+}$ fragment ions.

Figure 2c shows the MS/MS spectrum of the $[M+Cu+2H]^{4+}$ complex. Two different fragmentation patterns (fragment "b" and "y" ion series) are found in the MS/MS spectrum of the $[M+Cu+2H]^{4+}$ complex like those for the $[M+Cu]^{2+}$ or $[M+Cu+H]^{3+}$ complex, while the fragment "a" ion series was not observed in the MS/MS spectrum of $[M+Cu+2H]^{4+}$. It is conjectured that the oxidative dissociation process induced by Cu ions was hindered by the $[M+Cu+2H]^{4+}$-altered geometry, which was caused by the two additive protons. New fragments of ⑦ $y_5$ and ⑧ $[b_{11}+Cu]^{2+}$ appear in Figure 2c. It is considered that the weak bonding characteristic at the E11-V12 peptide bond was newly created as a result of the geometric transition in $[M+Cu+2H]^{4+}$. The fragment ions observed are listed in Table S1.

**MS/MS Spectra of (Aβ16 dimer—Cu)**

Both covalent and non-covalent bond dissociation were indicated by the MS/MS spectra of the (Aβ16 dimer—Cu) complex (Figure 3). During noncovalent bond dissociation, the $[D+Cu+3H]^{5+}$ complex was separated into three components: $[M+Cu+H]^{3+}$, $M^{3+}$, and $M^{2+}$, as shown in Figure 3a. Curiously, the $[M+Cu]^{2+}$ fragment ion (a counter ion of $M^{3+}$) was not observed in the $[D+Cu+3H]^{5+}$ non-covalent dissociation process. Three subunits were also produced in the $[D+Cu+H]^{3+}$ non-covalent dissociation process, $[M+Cu]^{2+}$, $M^{2+}$, and $M^{1+}$, which produced distinctive peaks (Figure 3b, $[M+Cu]^{1+}$ *m/z* 2014.8 is beyond the *m/z* range of our MS/MS spectrum).

In the covalent bond dissociation of the $[D+Cu+3H]^{5+}$ complex, {M + ①, ②, ③, or ⑤} fragment ions (Table 1) were observed as forms of the {M + fragment ions of $[M+Cu+H]^{3+}$}. The {①, ②, ③, and ⑤} ions are characteristic fragment ions resulting from the dissociation of

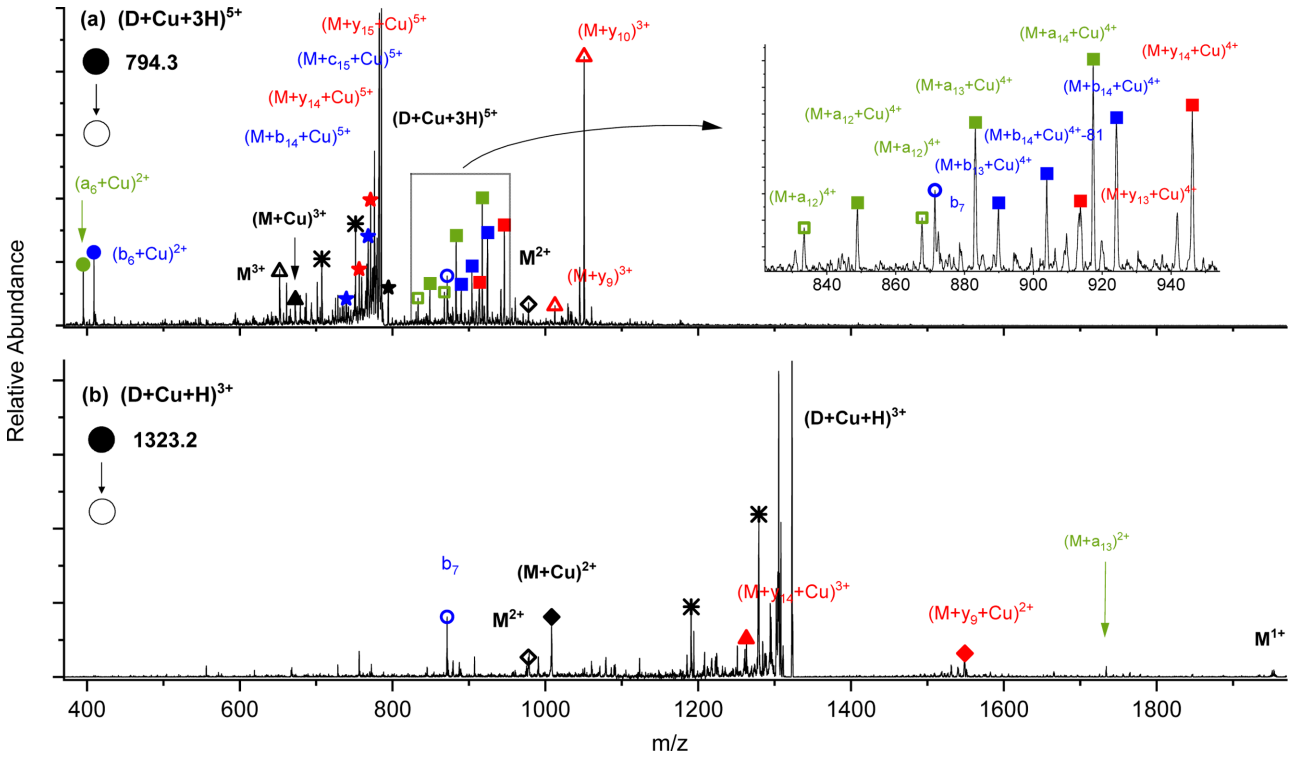


**Figure 3.** MS/MS spectra of (a) $[D+Cu+3H]^{5+}$ and (b) $[D+Cu+H]^{3+}$ parent ions. The charge states are distinguished by different shapes (1+ = circle, 2+ = diamond, 3+ = triangle, 4+ = square, 5+ = star). The a, b, and y fragment ions are indicated by green, blue, and red colors, respectively. The empty and filled shapes indicate the existence of Cu ions in the fragment ions. The asterisk ions are the fragment ions resulting from the (1+) ions stored at the same time as the $[D+Cu+3H]^{5+}$ or $[D+Cu+H]^{3+}$ parent ions in the LTQ ion trap.

$[M+Cu+H]^{3+}$ (Table 1). The {①, ②, ③, and ⑤} fragment ions were not observed in the MS/MS spectrum of the Aβ16 (3+) monomer ($M^{3+}$).[20] Therefore, the $[D+Cu+3H]^{5+}$ complex structure was deduced to form a {monomer-[monomer-Cu]} geometry, which has the possibility to conserve the original Cu coordination geometry of the $[M+Cu+H]^{3+}$ component. In the form of the {monomer-Cu-monomer} geometry, the original Cu coordination would be affected by the second Aβ16 monomer. Schematic $[D+Cu+3H]^{5+}$ structures are proposed for the {M-M-Cu} geometry in Schemes 1b and 1c, corresponding to the {M + ①, ②, or ③} and {M + ⑤} fragment ions, respectively. The fragment forms of the {M + fragment ions of $[M+Cu+2H]^{4+}$}, {M + ⑦ or ⑧}, are not observed in Figure 3a. Therefore, we believe that there is a preference for the $\{M^{2+}+[M+Cu+H]^{3+}\}$ geometry over the $\{M^{1+}+[M+Cu+2H]^{4+}\}$ geometry in the [Aβ16 dimer—$Cu]^{5+}$ complex.

In the case of the MS/MS spectrum of the $[D+Cu+H]^{3+}$ complex, the {M + fragment ions of $[M+Cu]^{2+}$} fragment forms, {M+ ③ $a_{13}$}, and {M+ ④ $[y_9+Cu]^{1+}$} fragment ions (Table 1), are observed as weak-intensity peaks in Figure 3b. The {③$a_{13}$ or ④$[y_9+Cu]^{1+}$} ion signal was not observed in the MS/MS spectrum of the Aβ16 monomer.[20] Therefore, the {M-M-Cu} geometry for $[D+Cu+H]^{3+}$ is also expected to be more favorable than the {M-Cu-M} geometry. The schematic $[D+Cu+H]^{3+}$ structure is proposed to have the {M-M-Cu} geometry in Scheme 1d, corresponding to the {M+ complex4 geometry of $[M+Cu]^{2+}$}.

## Conclusion

CID-MS/MS experiments were conducted to obtain structural information regarding the (Aβ16 dimer—Cu) complex. Schematic $[D+Cu+3H]^{5+}$ structures (Schemes 1b and 1c) are proposed based on the {M + ①, ②, ③, or ⑤} fragment ions, which have the form of {M + fragment ions of $[M+Cu+H]^{3+}$} instead of the form of {M + fragment ions of $[M+Cu+2H]^{4+}$}. The Scheme 1d geometry of the $[D+Cu+H]^{3+}$ complex is expected to be more favorable than the geometries of Schemes 1b an 1c. The Scheme 1d structure is proposed for the $[D+Cu+H]^{3+}$ complex, based on the {M + ④ $[y_9+Cu]^{1+}$} fragment ions, which have the form of the {M+ complex4 geometry of $[M+Cu]^{2+}$}.

## Acknowledgments

This study was supported by the Kumoh National Institute of Technology (2021).

 

## Notes and references

Electronic Supplementary Information (ESI) is available [Table S1 and Figure S1]. See DOI: 10.5478/MSL.2023.14.4.153

## References


1. Chiti, F.; Dobson, C. M. *Annu. Rev. Biochem.* **2006**, 75, 333. https://doi.org/10.1146/annurev.biochem.75.101304.123901
2. Shankar, G. M.; Walsh, D. M. *Mol. Neurodegener.* **2009**, 4, 48 https://doi.org/10.1186/1750-1326-4-48
3. Haass, C.; Schlossmacher, M. G.; Hung, A. Y.; Vigo-Pelfrey, A.Mellon, B. L. Ostaszewski, I. Lieberburg, E. H. Koo, C.; Schenk, D.; Teplow, D. B.; Selkoe, D. J.; *Nature*, **1992**, 359, https://doi.org/10.1038/359322a0
4. Hardy J.; Selkoe, D. J.; *Science,* **2002**, 297, 353 https://doi.org/10.1126/science.1072994
5. Klein, W. L.; Stine, W. B.; Teplow, D. B. *Neurobiol. Aging* **2004**, 25, 569 https://doi.org/ 10.1016/j.neurobiolaging.2004.02.010
6. Benilova, I.; Karran, E.; De Strooper, B. *Nat. Neurosci.* **2012**, 15, 349 https://doi.org/ 10.1038/nn.3028
7. Pujol-Pina, R.; Vilaprinyó-Pascual, S.; Mazzucato, R.; Arcella, A.; Vilaseca, M.; Orozco, M.; Carulla, N. *Scientific Reports* **2015,** 5, 14809 https://doi.org/ 10.1038/srep14809
8. Ono, K.; Condron, M. M.; Teplow, D. B. *Proc. Natl. Acad. Sci. U.S.A.* **2009**, 106, 14745 https://doi.org/10.1073pnas.0905127106
9. Paravastu, A. K.; Leapman, R. D.; Yau, W.-M.; Tycko, R. *Proc. Natl. Acad. Sci.* **2008**, 105, 18349 https://doi.org/10.1073pnas.0806270105
10. Zou, Y.; Qian, Z.; Chen, Y.; Qian H.; Wei, G.; Zhang, Q. *ACS Chem. Neurosci.* **2019**, 10, 1585 https://doi.org/10.1021/acschemneuro.8b00537
11. Lovell, M. A.; Robertson, J. D.; Teesdale, W. J.; Campbell, J. L.; Markesbery, W. RS.; *J. Neurol. ci.,* **1998,** 158, 47
12. Sayre, L. M.; Perry, G.; Smith, M. A.; *Curr. Opin. Chem. Biol.,* **1999,** 3, 220 https://doi.org/10.1016/S1367-5931(99)80035-0
13. Smith, D. G.; Cappai, R. Barnham, K. J.; *Biochim. Biophys. Acta*, **2007**, 1768, 1976 https://doi.org/10.1016/j.bbamem.2007.02.002
14. Atwood, C. S.; Moir, R. D.; Huang, X.; Scarpa, R. C.; Bacarra, N. M.; Romano, D. M.; Hartshorn, M. A.; Tanzi, R. E.; Bush, A. I.; *J. Biol. Chem.,* **1998**, 273, 12817 https://doi.org/10.1074/jbc.273.21.12817
15. Guilloreau, L.; Combalbert, S.; Sournia-Saquet, A.; Mazarguil, H. and Faller, P.; *ChemBioChem*, **2007**, 8, 1317–1325 https://doi.org/ 10.1002/cbic.200700111
16. Brzyska, M.; Trzesniewska, K.; Wieckowska, A.; Szczepankiewicz, A. and Elbaum, D.; *ChemBioChem*, **2009**, 10, 1045 https://doi.org/ 10.1002/cbic.200800732
17. Zou, J.; Kajita, K.; Sugimoto, N.; *Angew. Chem., Int. Ed*., **2001**, 40, 2274 https://doi.org/10.1002/1521-3773(20010618)40:12<2274::AID-ANIE2274>3.0.CO;2-5
18. Raman, B.; Ban, T.; Yamaguchi, K.; Sakai, M.; Kawai, T.; Naiki, H.; Goto, Y.; *J. Biol. Chem*., **2005**, 280, 16157 https://doi.org/10.1074/jbc.M500309200
19. Lu, Y.; Prudent, M.; Qiao, L.; Mendez, M. A.; Girault, H. H.; *Metallomics***, 2010**, 2, 474 https://doi.org/10.1039/c004693k
20. Kim, K. M.; Kim, H.-T.; *Mass Spectrometry Letters*, **2022,** 13, 177 https://doi.org/10.5478/MSL.2022.13.4.177
21. Ke, Y.; Zhao, J.; Verkerk, U. H.; Hopkinson, A. C.; Siu, K. W. M.; *J. Phys. Chem. B*, **2007**, 111, 14318 https://doi.org/10.1021/jp0746648
22. Qiao, L.; Bi, H.; Busnel, J.-M.; Waser, J.; Yang, P.; Girault, H. H.; Liu, B.; *Chem. Eur. J.*, **2009**, 15, 6711 https://doi.org/10.1002/chem.200802229
23. Ganisl, B.; Valovka, T.; Hartl, M.; Taucher, M.; Bister, K.; Breuker, K.; *Chem. Eur. J.,* **2011,** 17, 4460 https://doi.org/10.1002/chem.201003709
24. Thompson, M. S.; Cui, W. D.; Reilly, J. P.; *Angew. Chem. Int. Ed.* **2004**, 43, 4791 https://doi.org/10.1002/anie.200460788
25. Kjeldsen, F.; Silivra, O. A.; Ivonin, I. A.; Haselmann, K. F.; Gorshkov, M.; Zubarev, R. A.; *Chem. Eur. J*. **2005**, 11, 1803 https://doi.org/10.1002/chem.201003709